Proceedings of 2020 IEEE Applied Signal Processing Conference (ASPCON)

# Measuring the Degree of Suitability of Edge Detection Operators Prior to an Application

Abhishek Kesarwani, Kiran Purohit, Mamata Dalui, and Dakshina Ranjan Kisku
*Department of Computer Science and Engineering*
*National Institute of Technology, Durgapur*
India
keabhi20@gmail.com, kiran.purohit789@gmail.com, mamata.dalui@cse.nitdgp.ac.in, and drkisku@cse.nitdgp.ac.in

***Abstract*—Unlike image restoration, image enhancement techniques are found to be subjective in nature as the appearance of an output image depends upon human perception. Hence, it is very difficult to determine the appropriateness of image enhancement techniques including edge detection operators prior to an application. This paper makes use of regression models to determine the suitability of edge detection operators before operators to be executed. With the existing operators, a novel Hybrid technique is used in the evaluation. The Hybrid detector is designed by combining Canny and Sobel operators with the gradient of texton image. This approach estimates a model as an objective function to determine the degree of proximity or suitability of edge detection operators under regression constraints on two publicly available databases, viz. the BSDS300 and the Multi-cue. The experimental results exhibit that the Hybrid edge detector outperforms other operators for measuring the proximity for appropriateness.**

***Index Terms*—Edge detection, Regression models, Filter bank, Pair disk mask, Image gradient.**

## I. Introduction

Edge detection [1] is an essential component of digital image processing. It plays a vital role in low-level feature extraction or finding shape information about objects. In edge detection, an edge is a sharp discontinuity change across gray level boundaries. This discontinuity may include a line, an isolated point or a corner point. Various image processing techniques can be used to identify edge points in an image where the brightness of the image changes more sharply and has discontinuities to observe. The construction of an edge depends on the optical and geometrical properties, noise level and illumination conditions of an image [2]. Edge detection operators are subjective in nature and there is no such basis function available to determine the best suitable edge detection operator prior to a particular application. Due to the subjective nature, it is very difficult to predict the optimal edge detector while the appropriateness of edge detection output to be decided visually as human perception varies from user to user. Moreover, a user perceives the outcome of edge detection function differently and decides the suitability after having some cognitive responses [3] generated from human vision system. Hence, it is cumbersome to obtain the same edged effect from a set of edge detection operators used for some specific application.

Edge detection performs major role in many vision and visual information processing related applications such as face recognition, medical imaging, remote sensing, robot vision, color image processing, industrial automation, computational biology, video processing, microscopic imaging, etc. Edges are determined to filter out relatively less basic and minute details, for improving the processing speed and bringing down the complexity without the loss of the necessary information. The edges acquired from non-trivial images are normally ruined by fragmentation. Therefore, the edge curves are frequently found disjoint due to the missing edge segments and these make the subsequent tasks of understanding the image data very complex. As a result, visual perception to understand the edges can prove to be a difficult task.

In order to determine the suitability of edge detection operators [1] such as Sobel, Canny, Prewitt, Roberts, Scharr, Laplacian and Hybrid edge detectors on diverse set of images prior to an application using regression models [4]–[6], the subjective nature of edge detection operators are transformed to objective functions while regression models compute the best-fit function for each operator.

In addition, determining the suitability of edge detection operators, this paper also proposes a novel edge detection method called Hybrid edge detector. It combines the weighted Canny edged image and weighted Sobel edged image with the texton gradient image [7], [8]. The novel edge detection operator is lined up with the existing operators for experiments while keeping the experimental protocol uniform for all operators. These edge detection operators exhibit sharp discontinuities after applying on an image and the edged effect which is obtained would be related to the structural information resulting appearance of the image to be changed.

The contribution of this paper is two-fold such as (a) report a novel edge detection operator called Hybrid operator and (b) to measure the degree of proximity (suitability) of edge detection operators using regression models prior to an application. The proposed approach reported in this paper is posed as building block of future applications where, in long run, the mechanism would serve the purpose of selecting first and second order derivative filters for building up new deep learning models prior to an application where convolution layer is an integrated part of it. Moreover, this work would change the perspective of seeing image enhancement techniques from subjective functions to objective ones. Further, in such applications where derivative filters are used frequently may have more selective options to have convenient and stable outcome. If image





ISBN: 978-1-7281-6882-1 PART: CFP20P52-ART

enhancement and segmentation qualities could be estimated prior to the prospective applications with specified filters, then it revolutionizes the objectives of the works in getting customized outputs according to users requirements.

The paper is organized as follows. Section 2 introduces the proposed Hybrid edge detection operator and the method to determine the suitability of edge detection operators. Section 3 presents database description, experimental results and analysis. Concluding remarks are made in the last section.

## II. Proposed Work

### A. Proposed Edge Detection Operator

In order to strengthen the process of detecting edges and sharp discontinuities for various image processing applications, a novel edge detection operator called Hybrid operator is proposed. It uses both Sobel [1] and Canny [1] detectors to provide high-frequency spatial information and at the same time, it normalizes the noise content in the image. Sobel edge detector uses approximation of gradient magnitude which gives efficient object boundaries and their orientations. It produces very sharp gradient approximations in high frequency discontinuities. Unlike Sobel operator, most edge detection operators do not give any emphasis on the pixels that are closer to the center of the mask. Canny operator extracts more edges than any other edge detection operators as well as it deals with noisy images by having Gaussian smoothing effect in the initial step. Moreover, only the dominant edge candidates in their neighborhood are considered as edges and less dominant candidates are discarded. That is why Canny operator is sometimes called non-maximum suppressor. Both Canny and Sobel operators works well on noisy images and extract edges even on smoothing conditions. On the contrary, other operators are unable to deal with high frequency discontinuities or noises present in images. Hence, the combination of Canny and Sobel operators used in Hybrid operator outperforms other combinations of edge detection operators. This rare combination makes the proposed operator very much useful for edge detection as well as image segmentation operations [9] while texture properties of the image is enhanced. In this operator, a texton based texture framework which gives a unique texture is used. This texton image [8] is created with the use of derivative of Gaussian [10] filter bank. Then we find the gradient of the texton image by the use of pair disk masks. The output image produced in this process is a combination of Canny operator, Sobel operator, and gradient of texton image.

The design process of the proposed operator consists of the following steps: (a) The first step constructs a derivative of Gaussian filter bank by convolving the Gaussian function [1] with the Sobel operator. Here, the Sobel operator is used as derivative operator. This derivative of Gaussian filter is computed at different scales ($\sigma_1 = 1.2$ and $\sigma_2 = 1.4$) and orientations (16 bins). With two different scales and 16 bins a filter bank of 32 filters is obtained. This pipeline of filters is then convolved with the input image and it creates a set of texton images while clustering is performed using k-means [11] with response values. It has been observed that if the kernel size varies then the overall appearance of convolution effect either turns to be smooth or contains high-frequency sharp discontinuities.

**Algorithm 1** PairDiskMask algorithm

**Input :** Radius, Orientation
**Output :** Pair Disk Masks
**procedure** PairDiskMask($radius, hdmOrientation$)
  $pdMasks = [\ ]$
  **for** <$radii = 1 : radius$> **do**
    $mask$ = `create matrix with all zero's having size` $(radii * 2 + 1, radii * 2 + 1)$
  **end for**
  **for** <$i = 1 : radii$> **do**
    $x = i - radii^2$
    **for** <$j = 1 : (radii * 2 + 1)$> **do**
      **if** $(x + (j - radii)^2 < radii^2)$ **then**
        $mask[i, j] = 1$
      **end if**
    **end for**
  **end for**
  $rotateAngle = 360.0/hdmOrientation$
  **for** <$i = 1 : hdmOrientation$> **do**
    $rotated$=`interpolate mask with` $-i * rotateAngle$
    $rotated[rotated{>}1]$=`1.0`
    $rotated[rotated{<}0]$=`0.0`
    $rotated\_p$=`interpolate mask with` $-i * rotateAngle - 180$
    ▷ Rotated Pair
    $rotated\_p[rotated\_p{>}1]$=`1.0`
    $rotated\_p[rotated\_p{<}0]$=`0.0`
    $pdMask \leftarrow rotated, rotated\_p$
  **end for**
  **return** $pdMask$
**end procedure**

**Algorithm 2** GetGradient algorithm

**Input :** Image, Pair Disk Mask
**Output :** Gradient image
$chi\_sqr\_dist = img * 0$
**for** <$i = 1 : num\_bins$> **do**
  $temp$ = `1 where` $img$ `is in` $bin$ $i$ `and 0 elsewhere`
  $g_i$ = `convolve` $temp$ `with left_mask`
  $h_i$ = `convolve` $temp$ `with right_mask`
  `update` $chi\_sqr\_dist += 0.5 \times \sum_{i=1}^{num\_bins} \frac{(g_i - h_i)^2}{(g_i + h_i)}$
**end for**

(b) Second step determines texton image and it is then quantized in terms of set of pixels having range of [1, k] where k represents the number of clusters in k-means clustering algorithm. To obtain a better result, k is fixed to 64. The filter bank produces a three-dimensional vector where depth is equal to the number of filters used. Further, the gradient of texton image is obtained with the help of a pair of masks as described in Algorithm 1. Here, the pair of disk masks refers to a pair of binary images of half disk. The pair of masks, i.e., left mask and right mask are convolved with an image having 0 and 1 pixel values where the pixel values are decided to be 1 when equal number of bins are found at the corresponding pixel locations and rest of the pixel locations are assigned to be 0. Then we find a distance between this two convolved images using Chi-square metric [12] which is found to be faster as compared to aggregating count and pixel neighborhood for the histogram as described in Algorithm 2. Algorithm 1 is used for generating Pair disk masks which is further used in the Algorithm 2 for generating the gradient image. The pair of masks is made to be determined with three scales (5,10,15) and 8 orientations that correspond to the radius of a disk. The size of a kernel varies with respect to the radius of a disk. (c) Third step computes a pair of edged images which are obtained by convolving the Canny



ISBN: 978-1-7281-6882-1 PART: CFP20P52-ART

and Sobel edge detectors with the input image. Then weighted edged images are determined by multiplying a weight with each edged image. Weights are determined according to the output it produces accurately. Further, weighted edged images are combined with the gradient of texton image as given in Equation(1).

$$O = Tg \times (w1 \times Canny\_image + w2 \times Sobel\_image) \quad (1)$$

where, $O$ is output image, $Tg$ is gradient of texton image, $w1$ and $w2$ are weights ($w1 + w2 = 1$). For this experimental setup, sobel image have more weightage than canny image as the output image need to be made sharper. Hence, the parameters $w1 = 0.3$ and $w2 = 0.7$ is suitable for this experiment. The design process of the proposed egde detection operator is shown in Fig. 1.

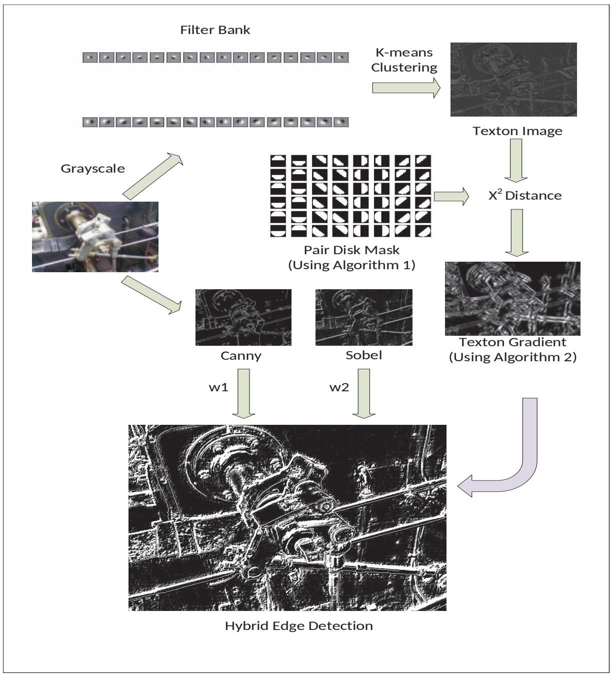


Fig. 1: Design Process of the Proposed Edge Detection Operator

### *B. Measuring Appropriateness of Edge Detection Operators*

This section presents a robust methodology to measure the degree of proximity of the edge detection operators using regression models [4]–[6]. In order to achieve the objective, the root mean square error (RMSE) [13] can be calculated for the respective edge detector. RMSE is directly related to the strength of the discontinuity in the image caused by the changes in the gray levels. In simple words, more the RMSE determined for an edge detector, more sharp the discontinuity to be found in the image. This helps us to choose mathematically the most optimal edge detector prior to an application. All the measures like RMSE, Mean Absolute Distance (MAD) and correlation coefficient, if applied directly, would not always produce correct proximity about appropriateness of an edge detection operator as all of them depend on the kernel values only. Some kernels have high values whereas some other have low values. So, in this case, for an edge detector, kernels having high value would be considered as best for detecting edges as RMSE, MAD and correlation coefficient measures are found to be higher than other edge detectors. However, it might not be the correct measure as sometimes edge detectors having higher RMSE, MAD and correlation coefficient measures would produce undesired output. To get rid of this unlikely situation, a mechanism needs to be devised under the constraints of regression models to find an optimal edge detection operator that measures the sharp discontinuity present in the image more accurately without overlapping with irrelevant information for a particular application. Therefore, a set of regression models such as linear, support vector, and multiple regression models are used. These regression models find an optimal best-fit function in the cloud of response values determined from individual edge detection operator. This optimal best-fit function is referred to as regression line, regression curve, and regression plane in case of linear, support vector, and multiple regression models respectively. This mechanism would be found useful when the suitability of the edge detection operator is being verified prior to an application. Moreover, this approach facilitates the entire process to transform a subjective image processing technique to an objective function where the dependency on the user's cognitive perspective is minimized.

Traditionally, edge detection operators are compared by means of visible perception of their output image. In case of non-trivial images, it is nearly impossible and unreliable to conclude which edge detection operator is best just by looking at the output provided by it. Also, the selection of an edge detector depends on the nature of edges. Therefore, it is imperative to determine the suitability of an edge detector prior to an application.

Some commonly used parameters are not suitable to determine the degree of proximity of an edge detector prior to an application. For, e.g.,

- Response value cannot be used as a parameter to determine the suitability of an edge detector as it is not a correct measure because some kernels have high values whereas some have low values.
- Total number of edges is also not a correct parameter to determine the suitability of an edge detector as false edges may occur due to noise [14].
- Visual perception [15] is also not a correct measure to determine the suitability of an edge detector as it is nearly impossible and unreliable to conclude which edge detection operator is best just by looking at the output provided by it.

Next, the regression models are introduced briefly with their working principles.

**Linear Regression:** In linear regression [4], one variable is considered as the independent variable (x) and the other is considered as the dependent variable (y). In this regression model, the square distance between the observations themselves and the predicted values are minimized as given in Equation (2).

$$Diff_i^2 = (y_i - (mx_i + c))^2 \quad (2)$$

where, $m$ is slope of a line and $c$ is intercept of a line.



ISBN: 978-1-7281-6882-1 PART: CFP20P52-ART

TABLE I: RMSE on BSDS300 dataset

| Edge Detector Operators | Linear Regression RMSE values | | | | | Support Vector Regression RMSE values | | | | | Multiple Regression RMSE values | | | | |
|---|---|---|---|---|---|---|---|---|---|---|---|---|---|---|---|
| | Image-1 | Image-2 | Image-3 | Image-4 | Image-5 | Image-1 | Image-2 | Image-3 | Image-4 | Image-5 | Image-1 | Image-2 | Image-3 | Image-4 | Image-5 |
| Sobel | 67.16 | 79.24 | 89.44 | 78.56 | 87.45 | 72.48 | 83.65 | 91.23 | 80.61 | 91.94 | 60.58 | 74.70 | 101.33 | 76.33 | 86.98 |
| Prewitt | 59.66 | 69.56 | 79.58 | 67.77 | 78.61 | 64.27 | 72.96 | 81.50 | 69.30 | 83.31 | 50.49 | 64.47 | 85.23 | 63.08 | 74.95 |
| Roberts | 28.82 | 30.59 | 48.14 | 40.66 | 37.56 | 31.25 | 31.73 | 52.54 | 44.10 | 38.83 | 21.71 | 29.53 | 37.09 | 29.31 | 19.68 |
| Scharr | 102.34 | 111.46 | 107.01 | 107.84 | 113.31 | 106.02 | 115.24 | 123.47 | 109.93 | 120.40 | 120.44 | 133.85 | 164.56 | 136.98 | 145.68 |
| Laplacian | 67.12 | 81.20 | 91.79 | 86.74 | 92.42 | 73.22 | 93.66 | 107.89 | 100.81 | 109.48 | 40.24 | 70.11 | 84.85 | 80.27 | 86.32 |
| Canny | 92.72 | 117.33 | 120.65 | 119.45 | 121.71 | 98.99 | 135.42 | 141.98 | 138.94 | 144.47 | 43.39 | 79.30 | 86.95 | 83.18 | 90.14 |
| Hybrid | 1904.81 | 2420.90 | 3113.05 | 2294.91 | 2432.38 | 1982.51 | 2504.75 | 3282.15 | 2396.15 | 2535.72 | 847.61 | 1273.96 | 1783.85 | 1130.62 | 1397.27 |

TABLE II: RMSE on Multi-cue dataset

| Edge Detector Operators | Linear Regression Mean of RMSE values of 20 images | | | | | Support Vector Regression Mean of RMSE values of 20 images | | | | | Multiple Regression Mean of RMSE values of 20 images | | | | |
|---|---|---|---|---|---|---|---|---|---|---|---|---|---|---|---|
| | Multi-cue Subject-1 | Multi-cue Subject-2 | Multi-cue Subject-3 | Multi-cue Subject-4 | Multi-cue Subject-5 | Multi-cue Subject-1 | Multi-cue Subject-2 | Multi-cue Subject-3 | Multi-cue Subject-4 | Multi-cue Subject-5 | Multi-cue Subject-1 | Multi-cue Subject-2 | Multi-cue Subject-3 | Multi-cue Subject-4 | Multi-cue Subject-5 |
| Sobel | 80.22 | 81.19 | 82.02 | 82.29 | 78.54 | 83.19 | 86.75 | 82.97 | 87.16 | 83.03 | 82.17 | 75.18 | 81.97 | 78.75 | 69.07 |
| Prewitt | 70.40 | 73.58 | 70.41 | 73.14 | 68.84 | 73.16 | 78.76 | 71.82 | 77.92 | 72.37 | 68.66 | 66.07 | 67.51 | 67.60 | 56.06 |
| Roberts | 39.27 | 46.71 | 32.70 | 33.23 | 33.88 | 41.29 | 50.45 | 33.59 | 34.83 | 35.79 | 47.46 | 37.48 | 27.05 | 27.83 | 26.05 |
| Scharr | 110.60 | 112.83 | 112.96 | 110.67 | 108.35 | 115.93 | 114.90 | 116.42 | 111.77 | 113.01 | 144.05 | 130.75 | 140.50 | 136.66 | 123.87 |
| Laplacian | 86.82 | 93.62 | 80.08 | 83.48 | 75.49 | 101.43 | 109.83 | 92.04 | 96.36 | 84.22 | 127.54 | 86.02 | 82.31 | 68.41 | 57.36 |
| Canny | 121.03 | 122.44 | 118.64 | 116.22 | 109.73 | 142.88 | 146.14 | 138.09 | 132.74 | 121.32 | 127.46 | 137.57 | 122.53 | 75.83 | 128.26 |
| Hybrid | 2451.29 | 2189.57 | 2374.61 | 2429.39 | 2503.49 | 2419.95 | 2213.87 | 2618.78 | 2632.04 | 2652.86 | 1444.44 | 1273.12 | 1317.54 | 1286.35 | 1114.34 |

**Support Vector Regression:** Support vector regression (SVR) [5] is used while working with continuous values instead of discrete values. Here, RBF (Radial Basis Function) is used which is a non-linear kernel. The kernel functions transforms the data into a higher dimensional feature space so that the linear separation can be performed.

**Multiple Regression:** Multiple regression [6] is the modification of linear regression. The variable which is to be predicted is called the dependent variable (y). The variables which are used to predict the value of the dependent variable are called the independent variables $(x_1, x_2, ..., x_n)$. The equation of multiple regression is given in Equation (3).

$$y = b_1x_1 + b_2x_2 + \quad + b_nx_n + c \tag{3}$$

where, $b_i$'s $(i = 1, 2, .., n)$ are known as the regression coefficients, and $c$ is the constant.

Here, two independent variables and one dependent variable are taken. Dependent variable is represented by the response values obtained after convolution of the input image with the edge detectors. The first independent variable is represented by the pixel number and the second independent variable as the local binary pattern (LBP) [16] of the input image. In the case of LBP, the $p-value < 0.05$ isolates the relationship between independent and dependent variable, which does not lead to multicollinearity. The LBP feature vector is also processed for machine learning classifiers such as face recognition or texture analysis because of its discriminative power and computational simplicity.

As the regression models always try to give the least square error with the help of optimal best-fit function, therefore it would be appropriate to use these models to measure the degree of proximity of individual edge detection operator.

The proposed work consists of the following steps.

**Step 1:** Histogram equalization [1] is applied to correct the contrast of the given gray scale input image.

**Step 2:** Apply edge detection operators such as Sobel, Prewitt, Roberts, Scharr, Laplacian, Canny, and Hybrid to the histogram equalized image and obtain convolved edged images. These images give low level features, edges and sharp discontinuities.

**Step 3:** Plot the response values of the convolved image for each edge detection operator.

**Step 4:** Take independent variable $x$ as the pixel number (1,2,3,...,n) and the dependent variable $y$ as the response values (value at each pixel). For multiple regression take the other independent variable $x_2$ as the local binary pattern of the input image.

**Step 5:** Apply linear regression, support vector regression and multiple regression on the output image.

**Step 6:** Calculate root mean square error for the respective edge detector.

**Step 7:** Compare the root mean square error among different edge detectors. An edge detector having highest root mean square error would be best suitable for the input image.

The overall idea behind the proposed methodology is reflected from the above steps and it would be advantageous to apply this mechanism while it would be difficult to measure the appropriateness of the appearance of an output image with human perception.

## III. Evaluation

The proposed methodology has been evaluated with two publicly available databases, such as the Berkeley Segmentation Data Set and Benchmarks 300 (BSDS300) [17], and the Multi-cue boundary detection dataset [18]. The BSDS300 database consists of 300 images and it is basically used for image segmentation and object detection. To conduct the experiment, 200 images are selected randomly. On the other hand, the Multi-cue dataset consists of 100 scenes and each scene is having 20 frame instances including left and right view. For experiment, 10 scenes, each containing 20 images, are considered.

**Experimental Results and Analysis:** The RMSE calculation is improvised for each edge detector using three different regression models as shown in Table 1 and Table 2. Both the tables show the results on restricted number of images as it is difficult to show all the results due to space constraint. RMSE is directly related to the strength of the discontinuity. This helps us to choose mathematically the most optimal edge detector prior to an application. It has been observed from


ISBN: 978-1-7281-6882-1 PART: CFP20P52-ART

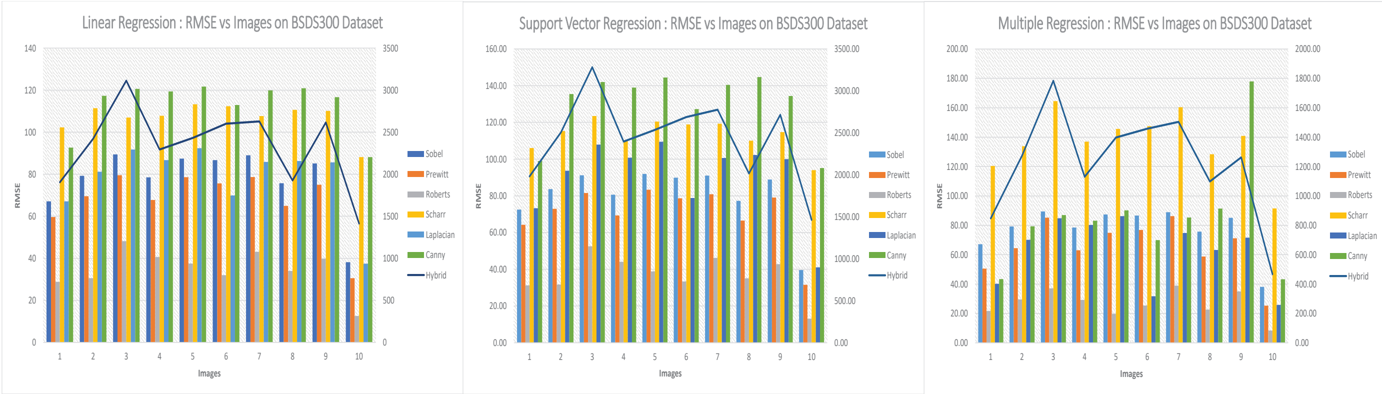


(a) Linear Regression on BSDS300 dataset (b) Support Vector Regression on BSDS300 dataset (c) Multiple Regression on BSDS300 dataset

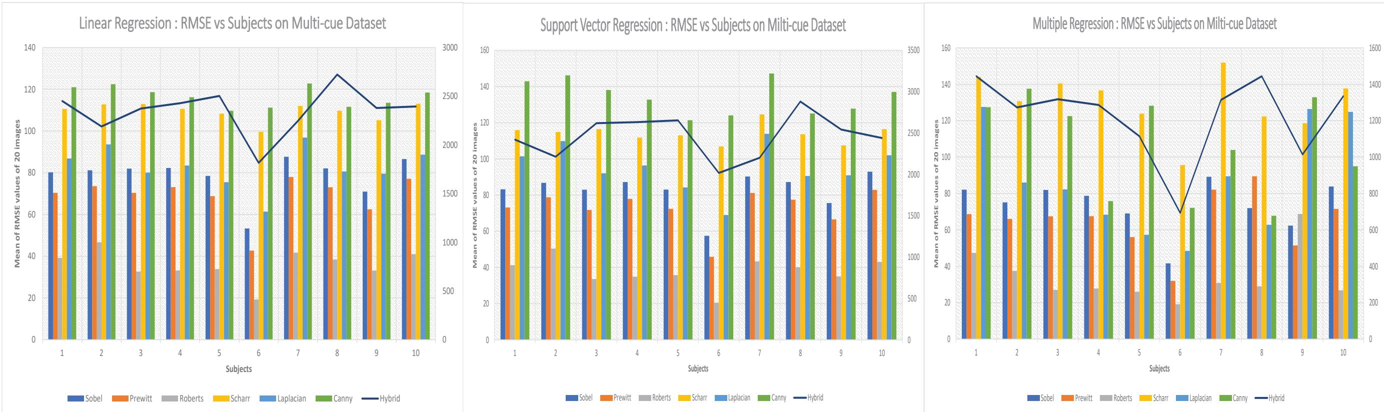


(d) Linear Regression on Multi-cue dataset (e) Support Vector Regression on Multi-cue dataset (f) Multiple Regression on Multi-cue dataset

Fig. 2: RMSE plot on BSDS300 and Multi-cue datasets

both the tables that the proposed edge detection operator is found dominating on both the datasets for all three regression models. In addition, it has also been observed that both Canny and Scharr operators alternately found suitable for many images in terms of degree of proximity. Also, Laplacian and Sobel performs closely identical in most of the cases. However, the degree of proximity for Hybrid edge detector is found significantly better than other operators. To show the regression enabled trade-off between RMSE and image using different sharpening filters, a pair of bar charts is made for each regression model determined on the BSDS300 and the Multi-cue datasets separately. To generate the bar chart, 10 images are taken from the BSDS300 dataset. Fig. 2 (a-c) shows three bar charts determined on the BSDS300 dataset for linear, support vector, and multiple regression respectively. From the Multi-cue dataset 200 images are taken from 10 scenes, i.e., 20 images from one scene. Fig. 2 (d-f) shows another three bar charts for the Multi-cue dataset for linear, support vector, and multiple regression respectively. Each bar chart appears to be a comparison between seven edge detectors that are validated through regression models. In order to have a better visualization of RMSE on different edge detectors two Y-axis are used. As the RSME for Hybrid filter (proposed one) is extremely high, all the edge detectors together in one axis cannot be observed. Therefore, two axes are required to show all the edge detectors in one bar chart. The left hand side Y-axis is for all edge detectors except Hybrid operator whereas the right hand side Y-axis is for Hybrid operator. It is clear from the bar charts that the Hybrid operator outperforms other edge detectors.

Fig. 3 (a-g) show the edged images obtained by applying Sobel, Prewitt, Roberts, Scharr, Laplacian, Canny and Hybrid operators respectively. It can be observed from the pictorial representations that the edged image obtained by Hybrid filter is found to have more prominent edges and sharp discontinuities than the edged images obtained by other edge detectors.

## IV. Conclusion and Future Scope

This paper has proposed a novel methodology to determine the appropriateness of edge detection operators using regression models. From the experiment, it has been observed that the Hybrid operator outperforms other edge detection operators with extremely high RMSE value. It is well known that an edge detection operator which gives higher RMSE value, would be considered as efficient edge operator. Although, in practice, regression models give least square error for consideration, however in the proposed work higher RMSE values are considered to determine the suitability of edge detection operators. Further, this work can be extended using deep learning models with integrated framework.



ISBN: 978-1-7281-6882-1 PART: CFP20P52-ART

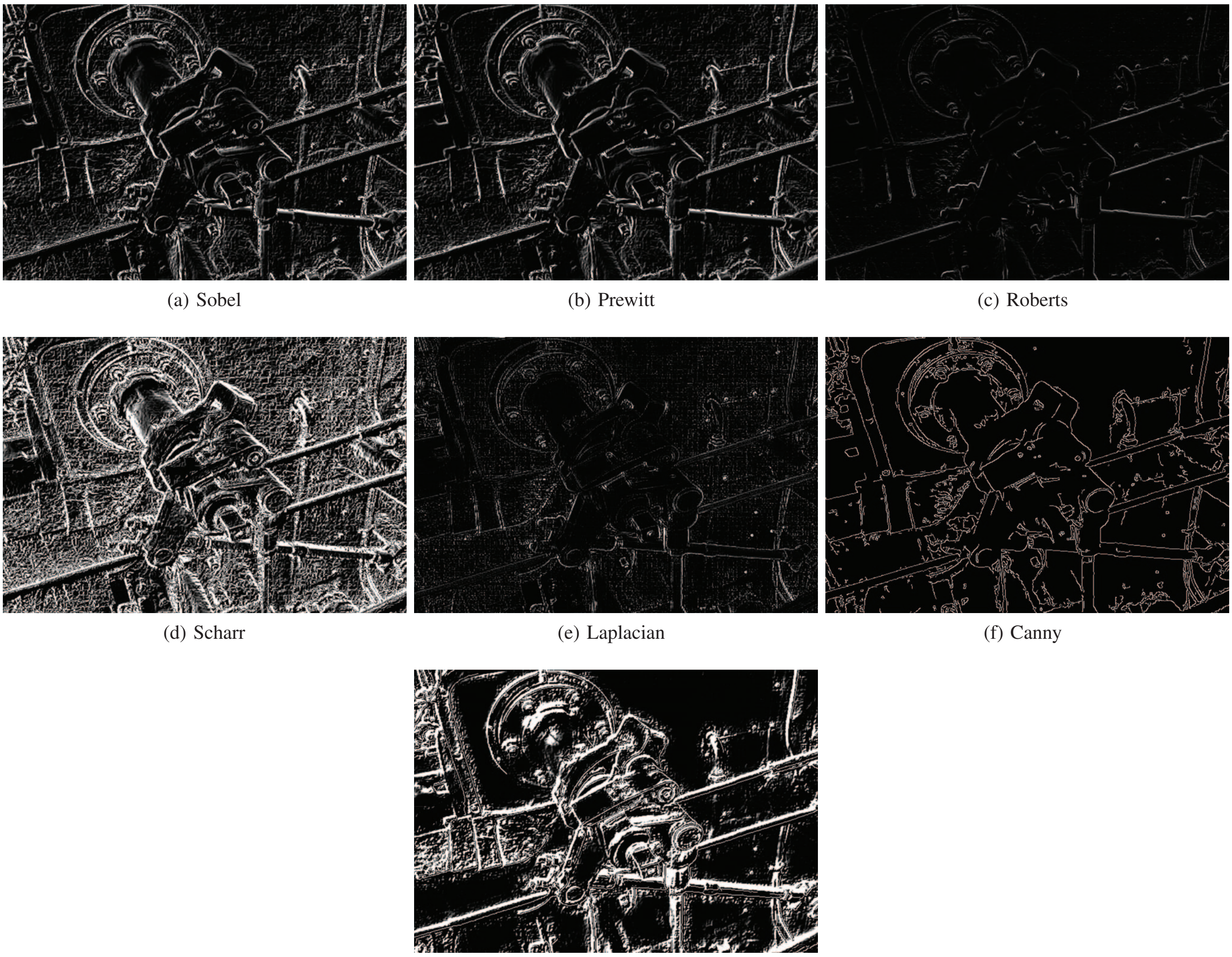

(a) Sobel (b) Prewitt (c) Roberts

(d) Scharr (e) Laplacian (f) Canny

(g) Hybrid

Fig. 3: Pictorial comparison of Hybrid filter with Sobel, Prewitt, Roberts, Scharr, Laplacian, and Canny filters

## REFERENCES


[1] R. C. Gonzalez, R. E. Woods, and S. L. Eddins, *Digital image processing using MATLAB*. Pearson Education India, 2004.

[2] H. Chidiac and D. Ziou, "Classification of image edges," in *Vision interface*, vol. 99, 1999, pp. 17–24.

[3] R. Petty, T. M. Ostrom, and T. C. Brock, *Cognitive responses in persuasion*. Psychology Press, 2014.

[4] D. C. Montgomery, E. A. Peck, and G. G. Vining, *Introduction to linear regression analysis*. John Wiley & Sons, 2012, vol. 821.

[5] A. J. Smola and B. Schölkopf, "A tutorial on support vector regression," *Statistics and computing*, vol. 14, no. 3, pp. 199–222, 2004.

[6] G. K. Uyanık and N. Güler, "A study on multiple linear regression analysis," *Procedia-Social and Behavioral Sciences*, vol. 106, no. 1, pp. 234–240, 2013.

[7] Q. Song, R. Xiong, D. Liu, Z. Xiong, F. Wu, and W. Gao, "Fast image super-resolution via local adaptive gradient field sharpening transform," *IEEE Transactions on Image Processing*, vol. 27, no. 4, pp. 1966–1980, 2018.

[8] C. He, S. Li, Z. Liao, and M. Liao, "Texture classification of polsar data based on sparse coding of wavelet polarization textons," *IEEE Transactions on Geoscience and Remote Sensing*, vol. 51, no. 8, pp. 4576–4590, 2013.

[9] A. Kalra and R. L. Chhokar, "A hybrid approach using sobel and canny operator for digital image edge detection," in *2016 International Conference on Micro-Electronics and Telecommunication Engineering (ICMETE)*. IEEE, 2016, pp. 305–310.

[10] B. Zhang, L. Zhang, L. Zhang, and F. Karray, "Retinal vessel extraction by matched filter with first-order derivative of gaussian," *Computers in biology and medicine*, vol. 40, no. 4, pp. 438–445, 2010.

[11] A. K. Jain, "Data clustering: 50 years beyond k-means," *Pattern recognition letters*, vol. 31, no. 8, pp. 651–666, 2010.

[12] X. Liu and D. Wang, "A spectral histogram model for texton modeling and texture discrimination," *Vision Research*, vol. 42, no. 23, pp. 2617–2634, 2002.

[13] N. Levinson, "The wiener (root mean square) error criterion in filter design and prediction," *Journal of Mathematics and Physics*, vol. 25, no. 1-4, pp. 261–278, 1946.

[14] Y. Liu, Z. Xie, and H. Liu, "An adaptive and robust edge detection method based on edge proportion statistics," *IEEE Transactions on Image Processing*, vol. 29, pp. 5206–5215, 2020.

[15] T. Cornsweet, *Visual perception*. Academic press, 2012.

[16] M. S. Karis, N. R. A. Razif, N. M. Ali, M. A. Rosli, M. S. M. Aras, and M. M. Ghazaly, "Local binary pattern (lbp) with application to variant object detection: A survey and method," in *2016 IEEE 12th International Colloquium on Signal Processing & Its Applications (CSPA)*. IEEE, 2016, pp. 221–226.

[17] D. Martin, C. Fowlkes, D. Tal, and J. Malik, "A database of human segmented natural images and its application to evaluating segmentation algorithms and measuring ecological statistics," in *Proc. 8th Int'l Conf. Computer Vision*, vol. 2, July 2001, pp. 416–423.

[18] C. Wojek, S. Walk, and B. Schiele, "Multi-cue onboard pedestrian detection," in *2009 IEEE Conference on Computer Vision and Pattern Recognition*. IEEE, 2009, pp. 794–801.




ISBN: 978-1-7281-6882-1 PART: CFP20P52-ART